LONG-TIME SIMULATIONS OF VORTEX SHEET DYNAMICS

BY DANIEL SOLANO[1], LING XU[2], AND SILAS ALBEN[2]

[1]Rutgers University, New Brunswick, NJ 08901, USA.
[2]University of Michigan, Ann Arbor, MI 48109, USA.

Abstract. We use unsteady two-dimensional vortex sheets to represent large-scale separated flows such as the vortex wake behind an airplane. In our computations, a continuous vortex sheet is approximated by an array of Lagrangian points whose motions are governed by the discretized Birkhoff-Rott integral. During the simulation, we use an Adaptive Mesh Refinement (AMR) technique to help resolve the dynamics of the vortex sheet; new points are inserted when adjacent Lagrangian points move far apart. However, the computational cost increases rapidly as more Lagrangian points are added. The aim of this work is to explore effective point insertion & deletion algorithms that make the computation efficient while maintaining sufficient accuracy of the vortex sheets to perform long time simulations.

Contents

1. Introduction 2
2. Birkhoff-Rott Equation 2
3. Vortex Roll Up Algorithm 3
4. Point Insertion Algorithm 5
4.1. Adaptive Mesh Refinement 1 5
4.2. Adaptive Mesh Refinement 2 6
4.3. AMR 1 Analysis 7
5. Point Deletion Algorithm (PDA) 7
5.1. Moment Conservation 7
5.2. Point Deletion Criterion 7
6. Additional Methods 10
7. Conclusion & Further Research 10
8. Acknowledgements 12
9. Bibliography 12
References 12

1. Introduction

Vortex Sheets are commonly used to model shear layers in fluid dynamics. An important application to Vortex Sheets is modelling an aircraft's wake, which induces drag on the aircraft producing the wake and is also hazardous for the next aircraft. A common practice is to replace a three-dimensional aircraft wake with a two-dimension fluid flow evolving over time such that the cross section of the three-dimensional aircraft wake corresponds to a specific time in the evolution of the two-dimensional fluid. Visually, the vortex sheet approximating the wake is a rolled up surface; this work models the vortex sheet cross section. In such aircraft wakes, the Reynold's number is very large, yielding negligible viscous forces. This work is concerned with modeling this type of two-dimensional incompressible, inviscid fluid for long periods of time using MATLAB©.

We denote $\boldsymbol{x} = (x, y)$ to be the displacement of a two dimensional fluid in $\mathbb{C}$ or $\mathbb{R}^2$ respectively. The velocity field

$$\frac{d\boldsymbol{x}}{dt} = \boldsymbol{u} = (u, v) = (\frac{dx}{dt}, \frac{dy}{dt})$$

of the fluid is a vector field on the fluid as a domain. The vorticity, ω, is the curl of the velocity field

$$\omega = \nabla \times \boldsymbol{u} = \frac{\partial v}{\partial x} - \frac{\partial u}{\partial y}$$

. The circulation Γ is essential to how the fluid model evolves:

$$\Gamma(x, y) = \int d\Gamma = \oint \boldsymbol{u}\, d\boldsymbol{l} = \int \omega(\boldsymbol{x'}) d\boldsymbol{x'}$$

2. Birkhoff-Rott Equation

The initial conditions corresponds to potential flow past a plate. The governing equation is the Birkhoff-Rott integral (2.1), yielding a coupled system of ordinary differential equations. This type of modelling has been studied carefully for medium-time simulations by R. Krasny in [1] "Computation of vortex sheet roll-up in the Trefftz plane".

$$\frac{d\bar{z}}{dt} = \frac{1}{2\pi i} \int \frac{d\Gamma'}{z - z'} \tag{2.1}$$

The complex congugate of the point $z = x + iy$ evolves according to the circulation of every point z, By Cauchy's theorem for Complex Integration, the only nonzero component of the integral will be the residues at the poles at z. So we define the Cauchy Kernel $K(z - z') = \dfrac{1}{2\pi i(z - z')}$.

Claim. In $\mathbb{R}^2$, the Birkhoff-Rott equation is equivalent to

$$\frac{dx}{dt} = \frac{1}{2\pi} \int_{P.V.} \frac{-(y - y')}{||\boldsymbol{x} - \boldsymbol{x'}||^2} d\Gamma' \qquad \frac{dy}{dt} = \frac{1}{2\pi} \int_{P.V.} \frac{(x - x')}{||\boldsymbol{x} - \boldsymbol{x'}||^2} d\Gamma'$$

Proof. First

$$\frac{d\bar{z}}{dt}(\Gamma,t)=\frac{1}{2\pi i}\int_{P.V.}\frac{d\Gamma'}{z-z'}\implies\frac{d\bar{z}}{dt}(\Gamma,t)=\frac{1}{2\pi i}\int_{P.V.}\frac{\bar{z}-\bar{z}'}{||z-z'||^2}d\Gamma'=$$

$$\frac{1}{2\pi i}\int_{P.V.}\frac{(x-iy)-(x'-iy')}{||z-z'||^2}d\Gamma'=\frac{1}{2\pi i}\int_{P.V.}\frac{(x-x')-i(y-y')}{||z-z'||^2}d\Gamma'=\frac{1}{2\pi}\int_{P.V.}\frac{-i(x-x')-(y-y')}{||z-z'||^2}d\Gamma$$

So

$$\frac{dz}{dt}(\Gamma,t)=\frac{dx}{dt}+i\frac{dy}{dt}=\frac{1}{2\pi}\int_{P.V.}\frac{-(y-y')}{||\boldsymbol{z}-\boldsymbol{z'}||^2}d\Gamma+i\cdot\frac{1}{2\pi}\int_{P.V.}\frac{(x-x')}{||\boldsymbol{z}-\boldsymbol{z'}||^2}d\Gamma$$

□

3. Vortex Roll Up Algorithm

In order to compute numerically, equation 2.1 is (1) desingularized, (2) parameterized, and (3) discretized. Computational singularities are avoided using a desingularized Cauchy Kernel $K_\delta(z-\tilde{z})$ yielding the equation:

$$\frac{d\boldsymbol{x}}{dt}=\frac{1}{2\pi}\int\frac{-(y-y')\boldsymbol{i}+(x-x')\boldsymbol{j}}{||\boldsymbol{x}-\boldsymbol{x'}||^2+\delta^2}d\Gamma'=\int K_\delta(\boldsymbol{x}-\boldsymbol{x'})d\Gamma.$$

As seen in [1], the line segment $l=\{(x,y)|x\in[-1,1],y=0\}$ (corresponding to the cross section of a plate) can be parameterized with an angle $\alpha\in[0,\pi]$ by defining $x,y,$ and Γ as functions of α. We then use a change of variables and set our bounds of integration to obtain the initial data:

$$\frac{d\boldsymbol{x}}{dt}=\int_0^\pi K_\delta(\boldsymbol{x}-\boldsymbol{x'})\frac{d\Gamma}{d\alpha}d\alpha\qquad\begin{array}{c}x(\alpha,0)=-cos(\alpha),\quad y(\alpha,0)=0\\ \alpha\in[0,\pi],\quad \delta\in(0,1],\ \Gamma=sin(\alpha)\end{array}$$

Define $\alpha_i=\pi\dfrac{i-1}{N}$, for $1\le i\le N+1$. We will consider vortices at $\boldsymbol{x_i}$ and for each i will express its velocity as the discretized integral sum of the effects the other vortices on that vortex. The integral is discretized by implementing a midpoint rule Riemann sum. Furthermore, $\boldsymbol{x_i}(t_{initial}+\Delta t)$ is determined by using a fourth order Runge Kutta method, which introduces the time step parameter Δt.

$$\frac{d\boldsymbol{x}_i}{dt}=\sum_{j=1}^{N}K_\delta(\boldsymbol{x}_i-\boldsymbol{x'}_j)\frac{d\Gamma}{d\alpha}\Delta\alpha_j\qquad\begin{array}{c}x_i=-cos(\alpha_i),\quad y_i=0\\ \text{RK4, Midpoint, }\Delta t\in(0,1],\ \Gamma=sin(\alpha_i)\end{array}$$

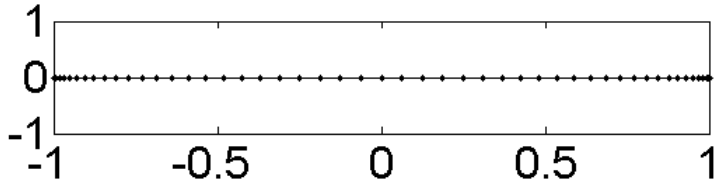

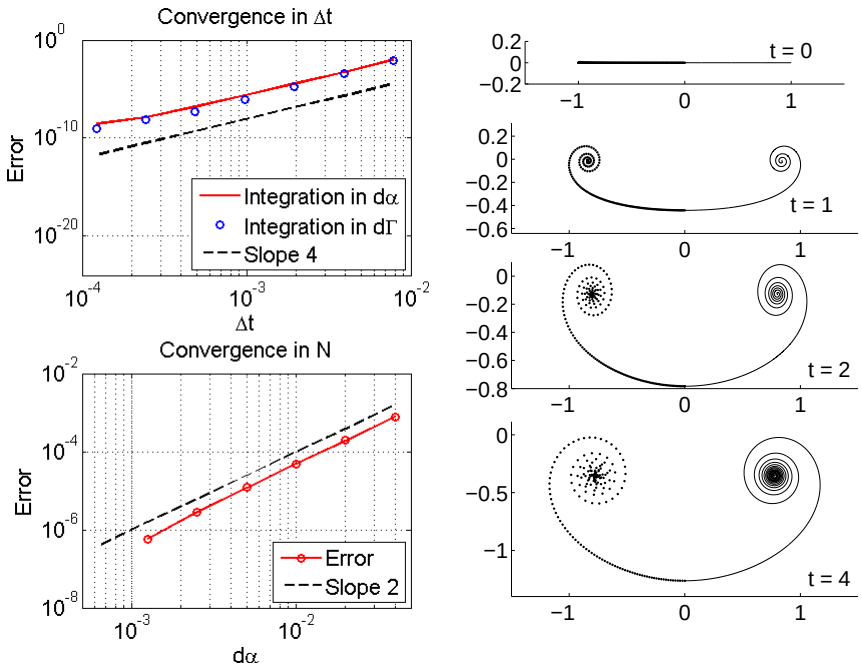

FIGURE 3.1. The Parameters N, Δt converge at the expected orders of 2 and 4. Initial time evolution results are shown.

The time evolution runs eqiuvalently using $\frac{d\Gamma}{d\alpha}\Delta\alpha_j \cong \Delta\Gamma_j$. In figure 3.1, the self-convergence with respect to Δt is of order 4, which is consistent with the expected order of convergence of the RK4 method; the self-convergence with respect to $N+1$ is also tested to have the proper order of 2 corresponding to the midpoint rule.

The initial results in figure 3.1 are identical to those of R. Krasny's in [1] with $N = 400$ $\delta = 0.05$, and $\Delta t = 0.01$. The smoothing parameter δ smears out the vorticity in the center of the spirals. The number of windings increases as $\delta \to 0$ as shown in figure 3.2.

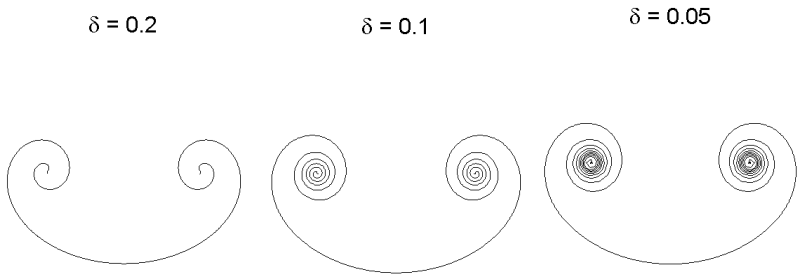

FIGURE 3.2. Node number $N = 1600$, $\Delta t = 0.1$, and $t_{end} = 5$

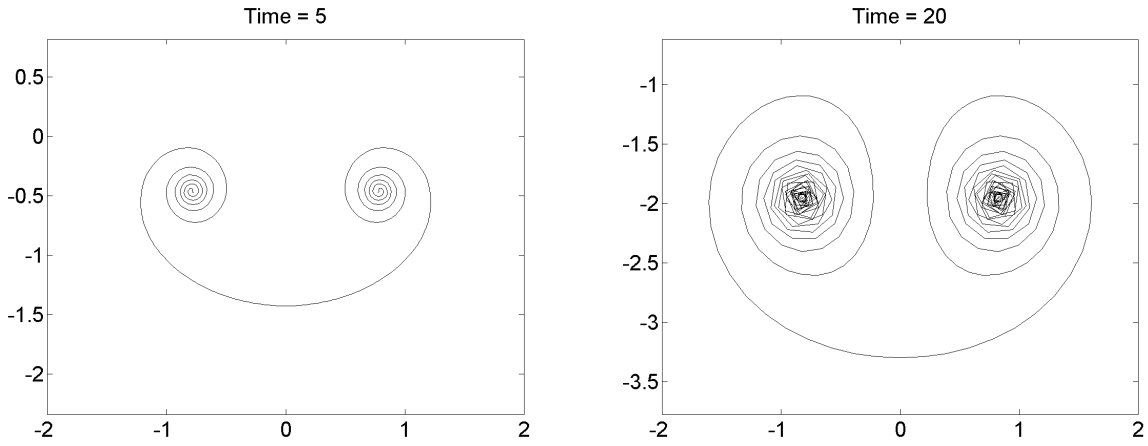

(A) (B)

FIGURE 3.3

The vortex sheet simulation accuracy is limited by the number of points $N+1$ as shown in Figure 3.3. As time increases, the vortex sheet length increases and thereby the distance between two points increases and the spiral becomes jagged. The jagged characteristic of the spiral is not due to instability, but due to a lack of resolution, ie, a lack of plotted data points. As a result, the "Point Insertion Algorithm" was implemented.

4. Point Insertion Algorithm

In this section the adaptive mesh refinement is implemented to increase N.

4.1. **Adaptive Mesh Refinement 1.** The AMR 1 criterion is the first and primary criterion to insert points; all points are restricted to be atmost ϵ_1 distance away from each other. Whenever there are two adjacent points $\boldsymbol{x_j}$ and $\boldsymbol{x_{j+1}}$that violate 4.1 we insert an $\alpha - space$ midpoint.

$$||\boldsymbol{x}_j - \boldsymbol{x}_{j+1}|| < \epsilon_1 \tag{4.1}$$

An $\alpha - space$ midpoint is found first by defining $\alpha_{new} = \dfrac{\alpha_j + \alpha_{j+1}}{2}$ and then using MATLAB's PCHIP cubic interpolation to find $\boldsymbol{x_{new}}$. The $\alpha - space$ interpolation is preferable to a spacial midpoint $\boldsymbol{x_{new}} = \dfrac{\boldsymbol{x}_j + \boldsymbol{x}_{j+1}}{2}$ since it yields a point on the curve of the solution vortex sheet as shown in figure 4.1, while the midpoint insertion, although computationally efficient, yields inaccuracy.

The spacial criterion parameter ϵ_1 is defined in terms of the smoothing parameter δ. Figure 4.1b compares the vortex sheet spiral center at $t = 50$ for $\delta = 0.2$, $\Delta t = 0.5$ and $N_{initial} = 100$ with no insertion, $\epsilon_1 = \delta/2$, $\delta/4$, and $\delta/8$.

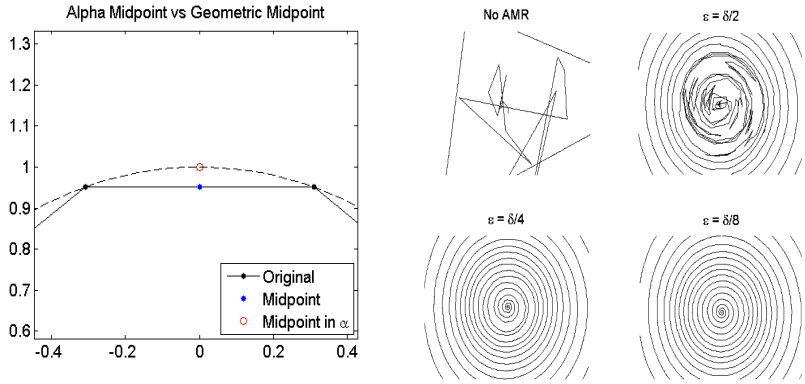

(A) (B)

FIGURE 4.1.
$$\begin{array}{ccc} (x,y) & \not\rightarrow_{midpoint} & (x_{new}, y_{new}) \\ \updownarrow & & \uparrow_{interpolation} \\ \alpha & \rightarrow_{midpoint} & \alpha_{new} \end{array}$$

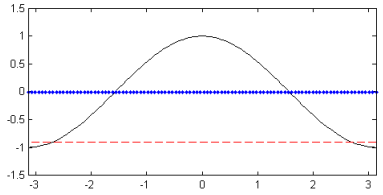

FIGURE 4.2. All angles θ_j that correspond to sections of the cosine plot above a horizontal line correspond to parts of the vortex sheet with excessive curvature.

4.2. **Adaptive Mesh Refinement 2.** Another criterion that may be useful to consider and discuss is an angular criterion. Define the angle θ_j between any two vectors $A = \boldsymbol{x_{j+1}} - \boldsymbol{x_j}$ and $B = \boldsymbol{x_{j-1}} - \boldsymbol{x_j}$. The criterion is that each θ_j must be less than some $0 \leq \theta_{CRIT} \leq \pi$. Intuitively, whenever the curvature is too great, ie the angle between A and B is too large, a point is inserted in the x_{j+1} place. The angle is indirectly evaluated via equation 4.2

$$\frac{A \cdot B}{||A|| \cdot ||B||} = \cos\theta_j. \tag{4.2}$$

For an example $cos\theta_j < 0$ corresponds to restricting $\theta_j < \pi/2$ and $cos\theta_j < -0.9$ corresponds to $\theta_j < 2.96$ so we choose different values for $cos\theta$ as shown in figure 4.2. As θ_j approaches π, the plot of the curve of the three points $\boldsymbol{x}_{j-1}$, $\boldsymbol{x}_j$, and $\boldsymbol{x}_{j+1}$ approaches linearity.

The point insertion was chosen to insert a point $\boldsymbol{x_n}$ between $\boldsymbol{x_{j-1}}$ and $\boldsymbol{x_j}$ using an $\alpha - space$ interpolation, however further study needs to be implemented on this criterion. Further thought

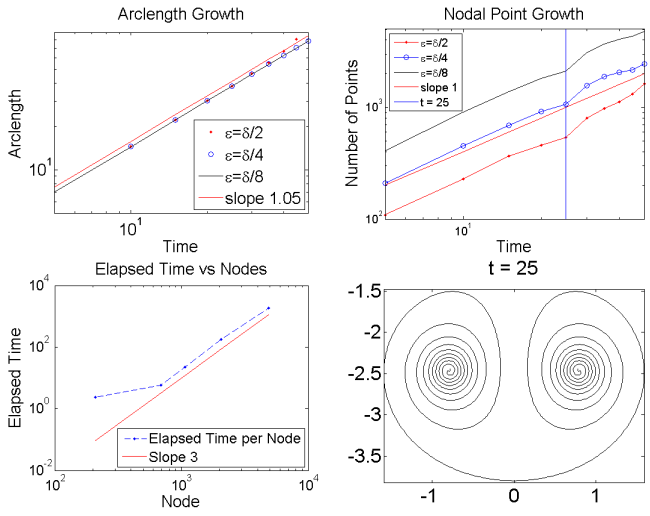

FIGURE 4.3. $\Delta t = 0.5$ and $\delta = 0.2$

may suggest a better way to insert points. This AMR criterion also requires the initial number of intervals N to be large in order to work properly.

4.3. **AMR 1 Analysis.** The arclength is shown to increase slightly fast than linearly in time. Further more nodal growth increases roughly linearly over time despite an odd kink in nodal growth at time $t = 25$. Most importantly, the Elapsed Time in seconds increases on an order of N^3, ie with slope 3 on the loglog scale. Because computational cost increases rapidly, a point deletion criterion must be considered

5. Point Deletion Algorithm (PDA)

5.1. **Moment Conservation.** Define the zeroth, first, and second moments of circulation for x_i, where $x_1 = x$ and $x_2 = y$ to be:

$$M_0 = \int_0^\pi d\Gamma, \qquad M_{1,i} = \int_0^\pi x_i d\Gamma, \qquad M_{2,ij} = \int_0^\pi x_i x_j d\Gamma \quad i,j = 1,2$$

In [2], it is proven that the zeroth moment, first moments, and the trace of second moment is conserved. So any Point Deletion Algorithm modeling the vortex sheet must conserve these momenta.

5.2. **Point Deletion Criterion.** The criterion implemented sets a lower bound ϵ_Γ to the $|\Delta\Gamma_j|$ of each interval between the nodal values. Intervals with negligible $|\Delta\Gamma_j|$ contribute very little to the time evolution since we integrate with respect to $\Delta\Gamma$.

$$|\Delta\Gamma_j| < \epsilon_\Gamma \implies \text{Negligible Contribution}$$

However in order to delete points, information of two intervals is considered, $|\tilde{\Delta}\Gamma| = |(\Gamma_{j+1} - \Gamma_j) + (\Gamma_j - \Gamma_{j-1})| < \epsilon_\Gamma$, in order to delete the point $\boldsymbol{x_j}$. Both Γ and $d\Gamma$ are plotted to visualize the curve segment between the horizontal lines $\pm\epsilon_\Gamma = \pm 10^{-4}$ that will be deleted.

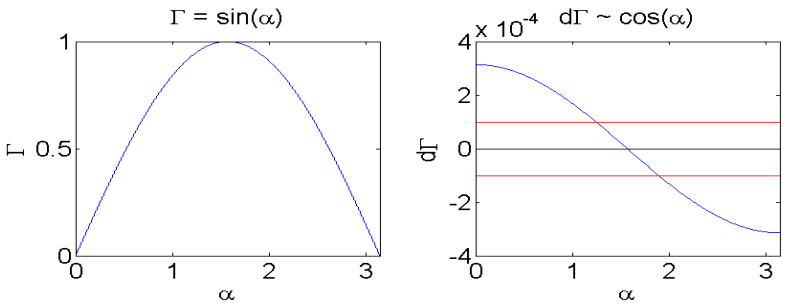

Nodal Growth Analysis. In figure 5.1, several different simulations with varying ϵ_Γ are compared via their nodal growth. When ϵ_Γ is large enough, the nodal growth is curtailed. For arbitrary periods of time t , its uncertain if the Point Deletion Algorithm will delete all points or too many points.

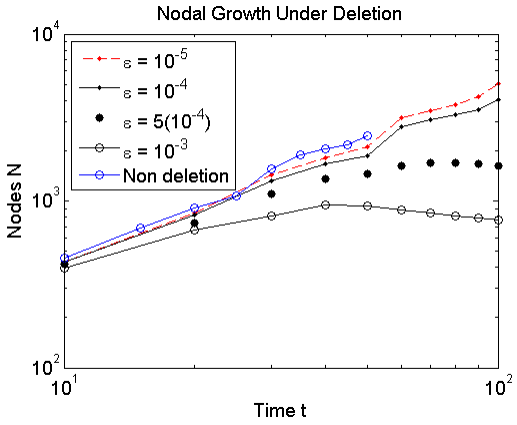

FIGURE 5.1. The ordinary point insertion algorithm and the point deletion algorithm with varying mesh deletion criterion, ie $\epsilon_\Gamma = 10^{-5}, 10^{-4}, 10^{-3}, 5 * 10^{-4}$, are plotted. Here we set $\epsilon_1 = \delta/4$ and $\Delta t = 0.5$.

The point deletion algorithm deletes large segments of the vortex sheet that do not carry large enough $|\tilde{\Delta}\Gamma|$ while still maintaining computational accuracy with respect to the the centers of the spirals. Conservation of the center spiral locations is demonstrated in figure 5.2, where with varying ϵ_Γ the plots are significantly different but the location of the center of the vortices are the same.

Momentum Conservation Analysis. The Point Deletion Algorithm was run until $t = 100$ with varying ϵ_Γ in order to compare the conservation of momenta. In figure 5.3, smaller ϵ_Γ yields smaller deviation over time with respect to momenta.

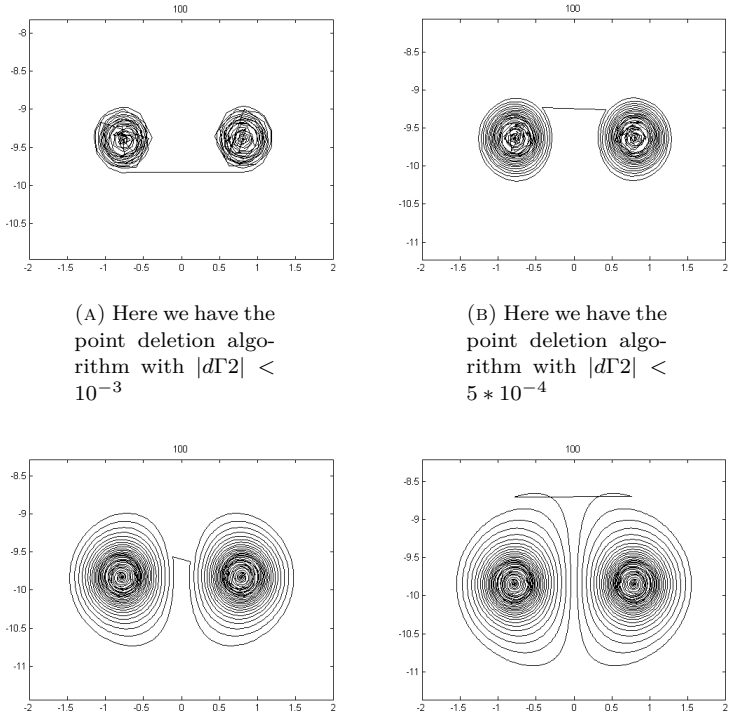

(A) Here we have the point deletion algorithm with $|d\Gamma 2| < 10^{-3}$

(B) Here we have the point deletion algorithm with $|d\Gamma 2| < 5 * 10^{-4}$

(C) Here we have the point deletion algorithm with $|d\Gamma 2| < 10^{-4}$

(D) Here we have the point deletion algorithm with $|d\Gamma 2| < 10^{-5}$

FIGURE 5.2. Here we analyze the plots of the vortex sheets that the requirement on $|d\Gamma 2|$ varies. Here we set $\epsilon_{DIS} = \delta/4$ and $\Delta t = 0.5$.

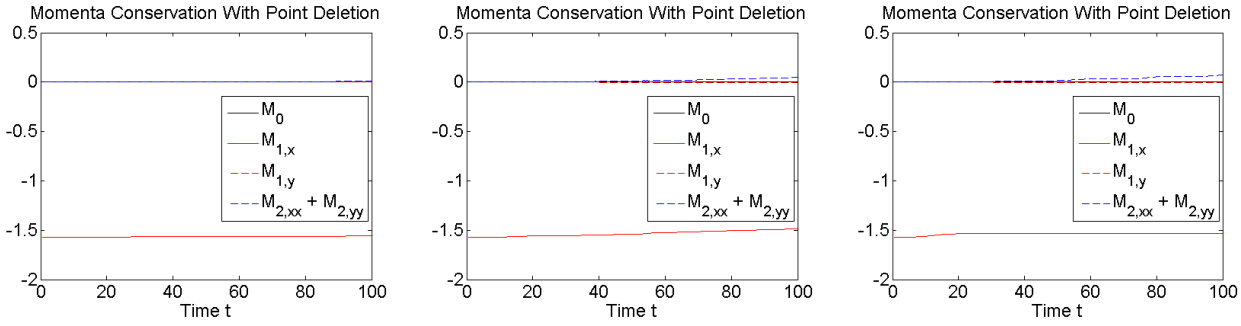

FIGURE 5.3. In the Momenta Conservation Plot, $\delta = 0.2$, $\Delta t = 0.5$ $\epsilon = \delta/32$ and $\epsilon_\Gamma = 10^{-4}, 5 \cdot 10^{-4}$, and 10^{-3}.

6. Additional Methods

Additional Methods were considered in order to set a maximum number of nodes since the behavior of the Point Deletion Algorithm with large enough ϵ_Γ at long times is uncertain. The PDA may begin deleting more points than it inserts, leading to a complete deletion of all point vortices. We implemented a maximum to the number of nodes allowed. Here we used $\Gamma = sin(\pi\alpha)$. Let $\epsilon_\Gamma = 10^{-4}$. Whenever the number of intervals N exceeded the maximum number of intervals N_{max}, then all points with $|\tilde{\Delta}\Gamma| < 10^{-3}$ are deleted

$$\text{If } N \leq N_{max} \text{ is violated } \implies \text{Delete all points with } |\tilde{\Delta}\Gamma| < 10^{-3}$$

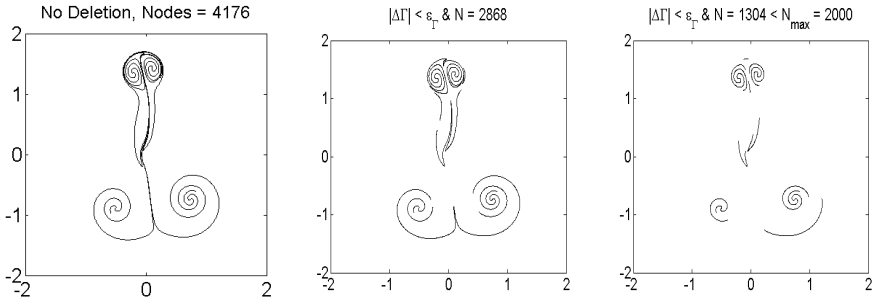

FIGURE 6.1. Here we show the vortex sheet corresponding to $\Gamma = sin(\pi \cdot \alpha)$, where $\alpha =\in [0, \pi]$, at $t = 5$ with no point deletion, point deletion, and a set maximum number of intervals.

In the first plot, no points are deleted, while the second plot, points are deleted according to the point deletion algorithm, and the third plot implements the maximum node method. Visually, large portions of the curve appear to have low contributions to the overall evolution of the curve. We implemented this maximal node method until time $t = 1000$ and plotted the momenta conservation, or lack there of in figure 6.2.

Further research must be developed to explore different options in curtailing nodal growth while maintain computational accuracy which is checked by the conservation of momenta.

7. Conclusion & Further Research

Modeling aircraft wakes using a distance based point insertion algorithm has been done before [1], however these models do not simulate for long time steps. The work presented in this paper demonstrate different ways to delete points for computational efficiency while maintaining a degree of computational accuracy. Further research must answer (1) how to delete points while conserving momenta and (2) which points are to be deleted. The criterion to determine which points are negligible must be improved in order to maintain computational accuracy. For possible leads, we analyze a histogram of the vortex sheet with $\Gamma = \sin(\alpha)$. The histogram of $|\Delta\Gamma|$ is plotted for times $t = 0, 2.5,$ and 5. Clearly, at time $t = 5$ in figure 7.1 there are many points being inserted in regions of low $|\Delta\Gamma|$.

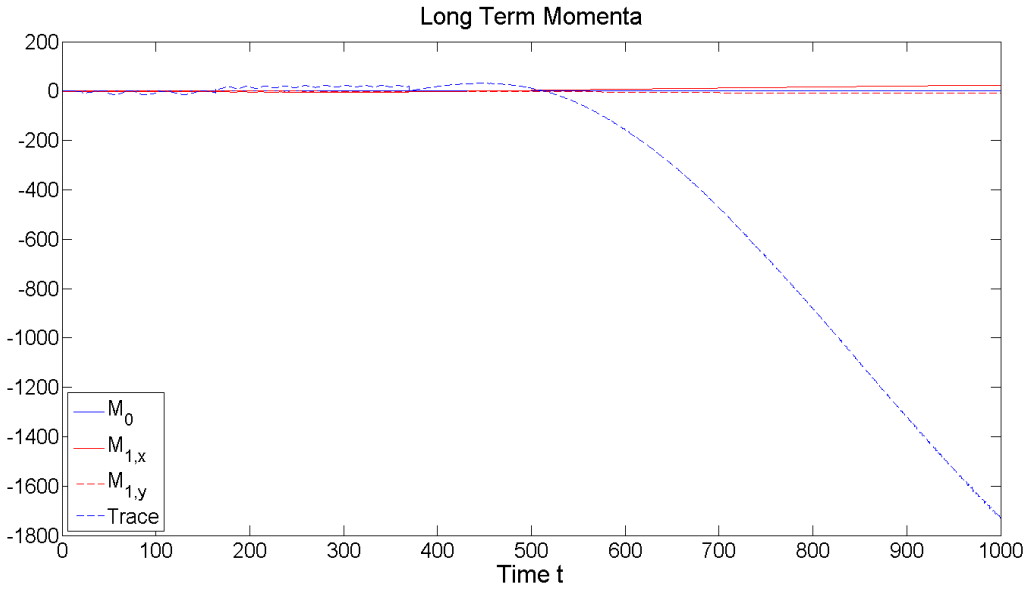

FIGURE 6.2. The moment oscillates about the original value until $Tr(M_2)$ decreases at $t = 500$.

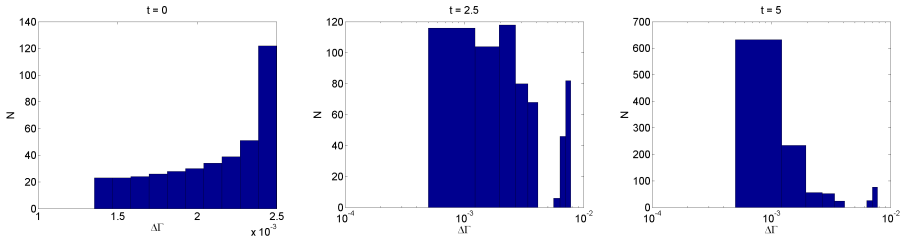

FIGURE 7.1. Here $N = 400, 621, 1101$ for each graph respectively

One possible direction is to not insert points in regions of the vortex sheet that contribute very little to the evolution of the sheet. Currently, the point insertion algorithm inserts points in regions with low $|\Delta\Gamma|$, as shown in the histogram plots. An explanation of this may be that the outer curves of the vortex spiral, that is, the sections of the vortex sheets that contribute little to the evolution, require many points to be inserted since they are physically long. A more efficient adaptive mesh refinement should be considered. AMR 2 may be worth investigating since it is based on the angle θ_j between to intervals; so sections of high curvature, such as the center of the spirals, would see more point insertion than sections of low curvature like the outer sections of the spirals. Another direction is to replace replacing spiral centers with point vortices. Note that $\dfrac{d\Gamma}{d\alpha} = s$, where s is the "strength" of vorticity, as commonly seen in literature [1]. Locating when

$$\frac{d^2\Gamma}{d\alpha^2} = 0 \tag{7.1}$$

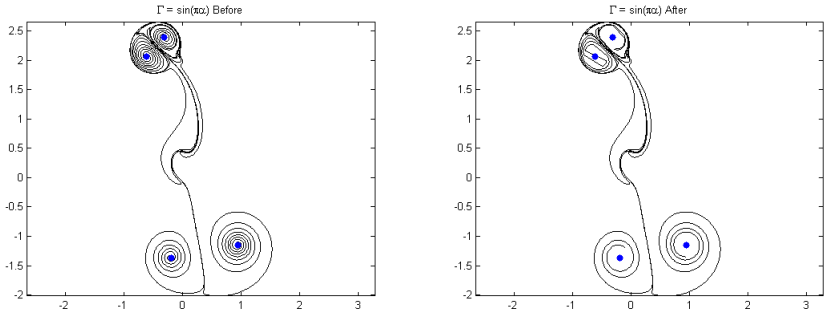

FIGURE 7.2. The vortex sheet corresponding to $\Gamma = sin(\pi\alpha)$ is plotted at $t = 10$. The centers of the spirals are found analytically using equation 7.1. All points within a radius r of each center are deleted.

is equivalent to finding the maxima and minima of vorticity. So another approach is to disregard the details of the center of the spiral, which winds up indefinitely, by replacing it with point vortices as shown in figure 7.2.

Further steps have been made to assign the momenta of the deleted points to their corresponding spiral center points to maintain momenta conservation. However a time evolution of this point absorption algorithm is under development.

8. Acknowledgements

I would like to thank Professor Ling Xu, whom I am indebted to for teaching and helping me master many numerical techniques required for this research and for meeting with me frequently. I would like to thank Professor Silas Alben for choosing me for this REU project this summer, for guiding this research, and for his incite on any road blocks I had or advice I needed. I would also like to thank Professor Robert Krasny for advice on how to model his work. I also like to thank the Department of Mathematics at the University of Michigan for giving me this outstanding opportunity to work in Ann Arbor and the National Science Foundation for providing the grant that made all of this project possible.

9. Bibliography

References

[1] R. Krasny, J. Fluid Mech. 184, 123 (1987)
[2] G. K. Batchelor, An Introduction to Fluid Dynamics (Cambridge University Press, New York, 2000)